Supplementary Material for

Facile synthesis of carbon quantum dots loaded with mesoporous g-C_3N_4 for synergistic absorption and visible light photodegradation of fluoroquinolone antibiotics

Yingfei Wang,[a] Fengliang Wang,[a] Yiping Feng,[a] Zhijie Xie,[a] Qianxin Zhang,[a] Xiaoyu Jin,[a] Haijin Liu,[b] Yang Liu,[c] Wenying Lv,[a] and Guoguang Liu*[a]

[a] School of Environmental Science and Engineering, and Institute of Environmental Health and Pollution Control, Guangdong University of Technology, Guangzhou, 510006, China

[b] School of Environment, Henan Normal University, Key Laboratory for Yellow River and Huaihe River Water Environment and Pollution Control, Xinxiang 453007, P. R. China.

[c] Faculty of Environmental & Biological Engineering, Guangdong University of Petrochemical Technology, Maoming, 525000, China

* **Corresponding Author**: Guoguang Liu

E-mail: liugg615@163.com

Phone: +86-20-39322547

Fax: +86-20-39322548

Address: School of Environmental Science and Engineering, Guangdong University of Technology, Guangzhou, Post Code: 510006, China

Test S1 Analysis methods

The concentrations of FQs in solution were analyzed using LC-20A high performance liquid chromatography (HPLC) (Shimadzu, Japan). The separation of FQs was performed with a Zorbax Eclipse XDB-C18 reversed phase column (4.6 x 150 mm, 5 μm). An isocratic elution, consisting of methanol and water, containing 0.2 % (v/v) formic acid at a flow rate of 1.0 mL/min. was used. The mobile phase composition and detection wavelengths can be found in Table S1. The injection volume was 20 μL. High-accuracy mass analyses of the intermediate byproducts were performed by HPLC/MS/MS (Agilent Technologies, USA) coupled with an Agilent 1100 series HPLC combined with a 6410 triple quadrupole mass spectrometer that used an Agilent SB-C18 column (5 μm, 4.6 x 150 mm). Elution was performed at a flow rate of 0.25 mL/min. With H_2O containing 0.1 % (v/v) formic acid as eluent A, and acetonitrile as eluent B; employing a linear gradient of from 10 % B to 60 % B in 15 min, and 60% B to 100% B in the next 2 min. Mass spectrometry analysis was conducted in positive mode using an electrospray ionization (ESI) source. The optimized parameters were as follows: fragmentor of 125 V; capillary voltage of 3.5 kV; desolvation gas (nitrogen, P 99.99 %), flow of 10 L/min; temperature of 350 ℃; nebulizer pressure of 40 psi; and scan range in full scan mode (m/z range 100-600). Once a potential product was identified, a product ion scan MS/MS was performed for the elucidation of the structure.

Table S1. Primary properties of water samples for FQs and substructural analogs.

Fluoroquinolones	Mobile phase composition		Detection wavelength (nm)
	H_2O (0.2% formic acid)	Me(OH)	
OFX	70%	30%	293
NOR	70%	30%	278
CIP	70%	30%	278
ENR	72%	28%	278
LOM	65%	35%	287
FLE	70%	30%	286

Table S2. Energy band structure parameters of g-C_3N_4, mpg-C_3N_4, and mpg-C_3N_4/CQDs

Photocatalysts	**X (eV)**	**E_c (eV)**	**E_g (eV)**	**E_{VB} (eV)**	**E_{CB} (eV)**
g-C_3N_4	4.72	4.50	2.66	1.55	-1.11
mpg-C_3N_4	4.72	4.50	2.58	1.51	-1.07
mpg-C_3N_4/CQDs	4.72	4.50	2.54	1.49	-1.05

Table S3. Absorption pseudo-second order model of OFX onto the mpg-C_3N_4 and mpg-C_3N_4/CQDs

Photocatalysts	**Qe (mg/g)**	**k (g/mg ·min)**	**R^2**
mpg-C_3N_4	9.3545	0.0027	0.9982
mpg-C_3N_4/CQDs	8.0128	0.0047	0.9984

Table S4. Mass spectrometry pieces information and proposed structure of photocatalytic products and OFX.

Number	Retention Time/min	ESI(+) MS (m/z)	ESI(+) MS/MS (m/z)	Supposed Structure
OFX	12.3	362	300,146	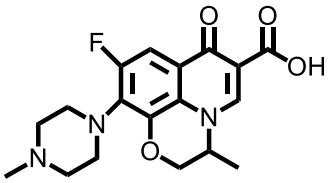
P1	7.2	260	243,147,129	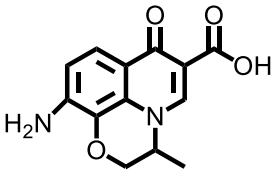
P2	7.5	304	289,260	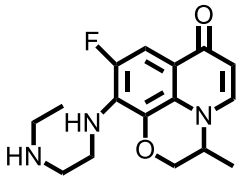 OR 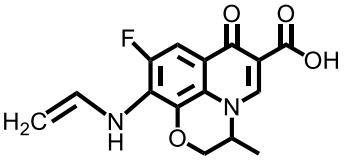
P3	7.9	312	272,244,228	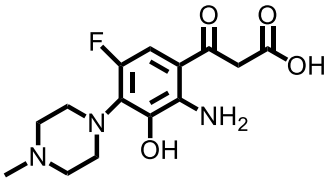
P4	8.1	348	327,302,261	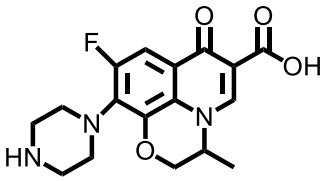
P5	8.7	278	233,208	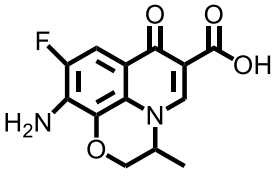

P6	9.1	391	374	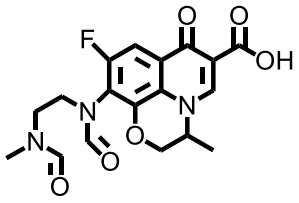
P7	11.0	326	268	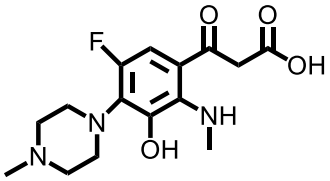
P8	11.4	354	283	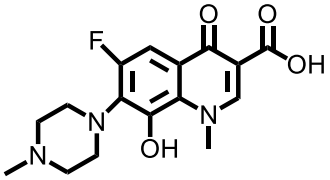
P9	12.1	318	300,256	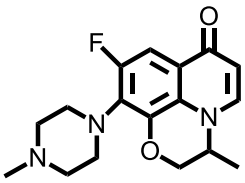

Table S5. Frontier electron densities on atoms of OFX calculated by using Gaussian 09 program at the B3LYP/6-311+g(d, p) level.

Atom (number)	$2FED^2_{HOMO}$	$FED^2_{HOMO}+FED^2_{LUMO}$	Point charge	Atom (number)	$2FED^2_{HOMO}$	$FED^2_{HOMO}+FED^2_{LUMO}$	Point charge
C(1)	0.0146	0.0159	0.1299	C(23)	0.0025	0.0601	-0.4170
C(2)	0.0471	0.0438	0.2014	C(24)	0.0010	**0.3289**	0.3002
C(3)	0.0423	0.0461	0.1788	F(26)	0.0028	0.0106	-0.2450
C(4)	0.0124	0.0139	0.1322	N(27)	0.0019	0.1138	-0.4845
N(9)	**0.2045**	**0.2053**	-0.3702	C(28)	0.0032	0.0135	0.0568
N(10)	**0.1718**	**0.1755**	-0.4699	O(29)	0.0039	0.0571	-0.3896
C(15)	0.0103	0.0262	0.0937	C(30)	0.0001	0.0229	**0.4242**
C(16)	0.0559	0.1388	0.1598	O(31)	0.0005	0.0255	-0.3707
C(17)	0.0218	0.0281	0.3547	O(32)	0.0001	0.0045	-0.0899
C(18)	0.0208	0.0266	-0.2351	C(34)	0.0063	0.0065	0.1363
C(19)	0.0034	0.0575	0.0249	C(39)	0.0003	0.0063	0.1557
C(20)	0.0190	0.0752	0.2774	C(43)	0.0004	0.0200	0.2918
C(21)	0.0013	0.0595	0.3725	O(46)	0.0157	0.0287	-0.3717

FIGURES

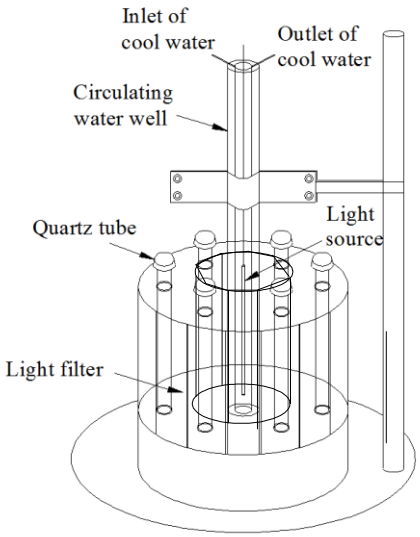

Fig. S1. Rotary photochemical reactor.

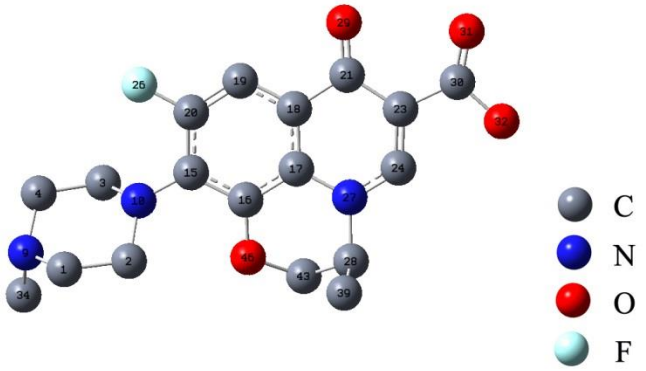

Fig. S2. Optimized structure and atomic numbering of OFX.

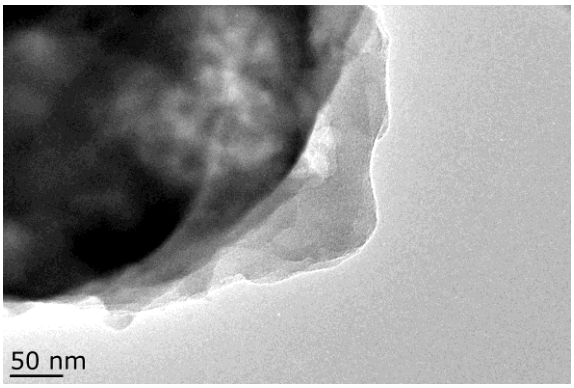

Fig. S3. TEM images of g-C_3N_4

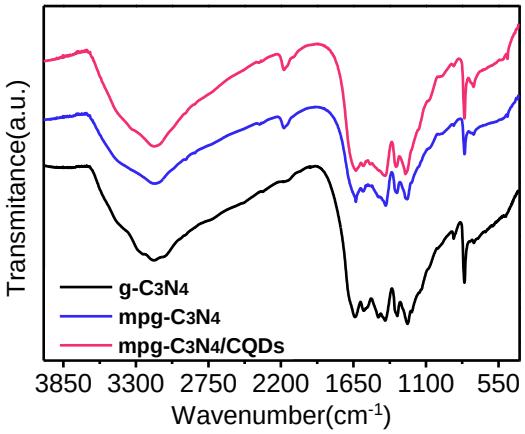

Fig. S4. FT-IR spectra of g-C_3N_4, mpg-C_3N_4, and mpg-C_3N_4/CQDs.

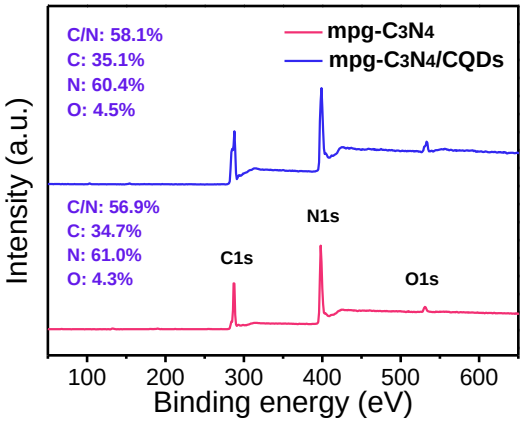

Fig. S5. XPS survey spectra of mpg-C_3N_4 and mpg-C_3N_4/CQDs.

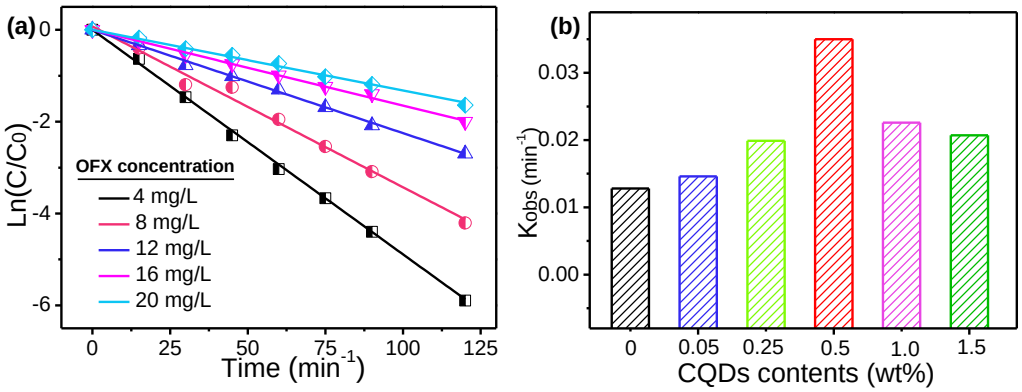

Fig. S6. (a) Effect of OFX initial concentration on the photocatalytic degradation kinetics of OFX; (b) loading amount of CQDs.

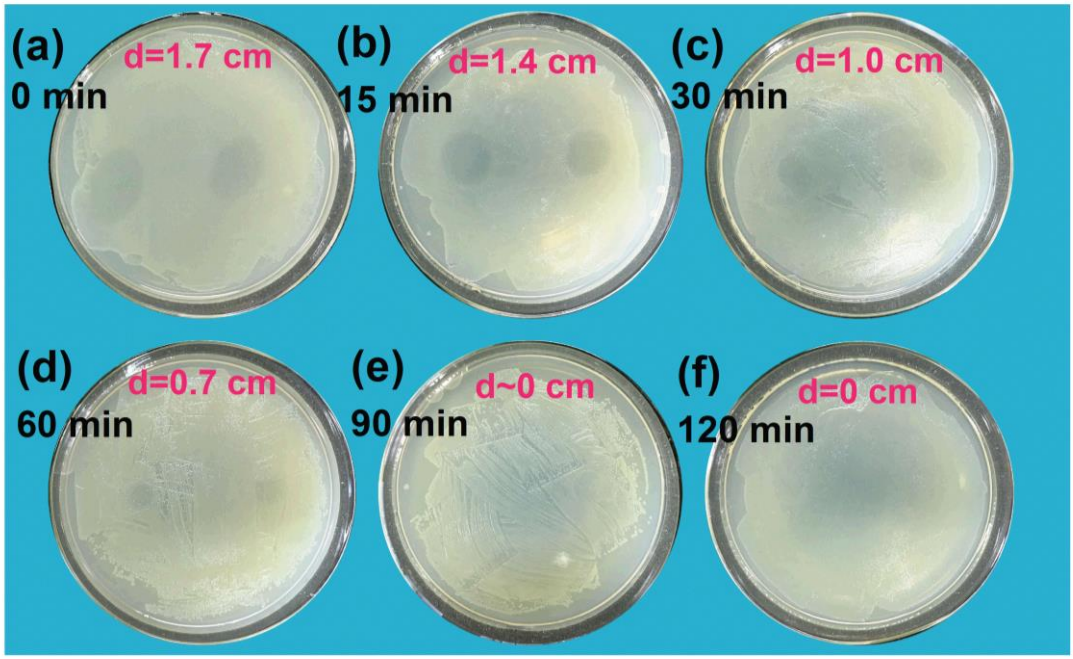

Fig. S7. Escherichia coli inhibition halo at different times of mpg-C_3N_4/CQDs photocatalytic reaction.